Geochemistry, Geophysics, Geosystems

Supporting Information for

Interplay of subduction tectonics, sedimentation, and carbon cycling

N. Riedinger[1], M. E. Torres[2], E. Screaton[3], E. A. Solomon[4], S. Kutterolf[5], J. Schindlbeck-Belo[6], M. J. Formolo[7], T. W. Lyons[8], P. Vannucchi[9,10]

[1]Boone Pickens School of Geology, Oklahoma State University, Stillwater, OK 74074, USA; corresponding author: natascha.riedinger@okstate.edu

[2]College of Earth, Ocean, and Atmospheric Sciences, Oregon State University, Corvallis, OR 97331, USA

[3]Department of Geological Sciences, University of Florida, Gainesville, Florida 32611, USA

[4]School of Oceanography, University of Washington, Seattle, WA 98195, USA

[5]GEOMAR Helmholtz Centre for Ocean Research Kiel, 24148 Kiel, Germany

[6]Institute for Geosciences, University of Heidelberg, 69120 Heidelberg, Germany

[7]ExxonMobil Upstream Research Company, Spring, TX, 77389, USA

[8]Department of Earth Sciences, University of California - Riverside, Riverside, California 92521, USA

[9]Earth Sciences Department, Royal Holloway, University of London, Egham TW20 0EX, UK

[10]Dipartimento di Scienze della Terra, Università degli Studi di Firenze, 50121 Firenze, Italy

Contents of this file

Additional information

Methane seeps

Although processes and mechanisms that lead to the expulsion of fluids and, consequently, the formation of seeps at the sediment surface are still under discussion, the main factors involved are considered to be specific tectonic settings/events and sediment composition and accumulation. The expulsion of hydrocarbon-rich fluids to the surface often occurs in pulses mainly related to changes in fluid flow (e.g., Hong et al., 2018). Such pulses can be caused, among others, by tectonic events, which can have an impact on the pressure and temperature of the underlying pore fluids as well as the properties of the fluids including viscosity (e.g., Leon et al., 2007; Sahling et al., 2008). The expelled fluids lead to specific structures at the sediment surface including seep precipitates, pockmarks, and mud volcanoes, which are strongly controlled by the rates and duration of fluid discharge as well as the chemical composition of the fluids (e.g., Bohrmann et al., 2002; Leon et al., 2007). The main process causing the formation of carbonates is microbially mediated anaerobic oxidation of methane (AOM; e.g., Boetius et al., 2000), which releases dissolved inorganic carbon (DIC) strongly depleted in ^{13}C and, consequently, the precipitation of ^{13}C-depleted carbonates (e.g., Peckmann et al., 2001; Aloisi et al., 2002).

Methane-derived authigenic carbonates

Our discussed carbon and oxygen isotope data from four selected samples from Unit II at Site U1379 are in good agreement with data previously reported to indicate near surface formation of carbonates and potentially influenced by gas hydrate occurrence (see also Gieskes et al., 2005; Han et al., 2014; Teichert et al., 2014, and references therein) (Fig. S1). The slight difference in the isotope data probably indicates lower AOM rates associated with the lower methane fluxes typically observed at the flanks of active methane discharge sites (Han et al., 2004; Hong et al., 2016, 2018). Hydrate dissociation is also responsible for more positive oxygen isotope values in the pore fluids (Hesse and Harrison, 1981)

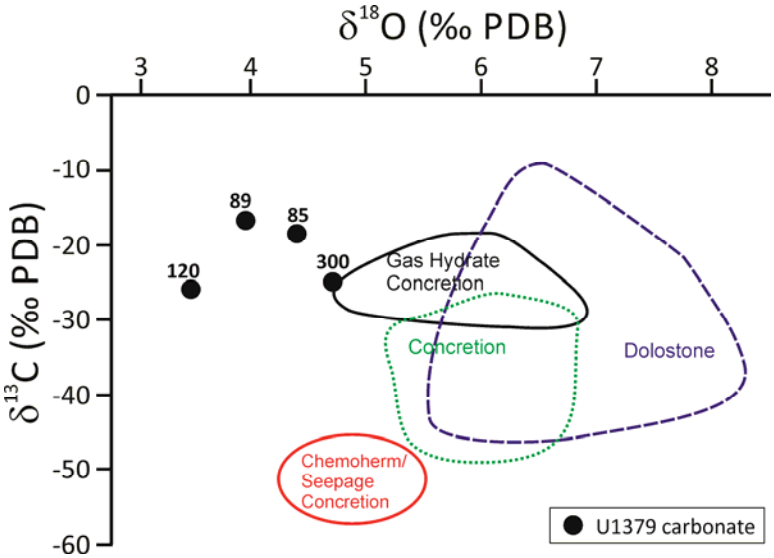

Figure S1 Carbonate carbon ($\delta^{13}C$) and oxygen isotopes ($\delta^{18}O$) data from Site U1379 plotted versus isotope data ranges of carbonate samples collected at the seafloor in the Costa Rican margin after Han et al. (2014).

Data availability

All geochemical data shown in the figures in the main text and generated onshore are provided in the tables below and are also available via the World Data Center PANGAEA. For method details and data accuracy/precision we refer to the method section in the main text. All data generated through the IODP Program are available through the IODP database LIMS.

Table S1. Pore water sulfate stable sulfur isotopes ($\delta^{34}S\text{-}SO_4$) and dissolved inorganic carbon (DIC) isotope ($\delta^{13}C$-DIC) data for the upper 80 m sediments at IODP 334 Hole U1378B.

Sample	Depth [mbsf]	$\delta^{34}S\text{-}SO_4$ [‰]	$\delta^{13}C$-DIC [‰]
U1378B 1H1	1.5	37.4	-4.34
U1378B 1H2	3	50.7	-12.74
U1378B 1H3	4.5	61.3	-10.76
U1378B 1H4	5.08	64.3	-14.12
U1378B 2H1	6.8	72.5	-15.45
U1378B 2H2	8.3	75.9	-18.62
U1378B 2H3	9.8	83.2	-19.85
U1378B 2H4	11.3		-22.35
U1378B 2H5	12.8		-21.91
U1378B 2H6	14.3		-16.45
U1378B 2H7	14.96		-14.08
U1378B 3H1	16.3		-8.57
U1378B 3H2	17.8		-5.35
U1378B 3H3	19.3		-1.67
U1378B 3H4	20.8		0.65
U1378B 3H5	22.3		2.92
U1378B 3H6	23.75		4.17
U1378B 3H7	24.5		5.08
U1378B 4H3	27.91		7.52
U1378B 4H6	32.41		6.77
U1378B 5H2	36.8		5.05
U1378B 5H6	42.8		4.11
U1378B 6H2	46.3		5.25
U1378B 6H5	50.8		6.13
U1378B 7H2	55.8		7.56
U1378B 7H5	60.3		8.12
U1378B 8H2	63.94		8.60
U1378B 8H5	68.44		8.49
U1378B 9H2	74.8		9.19
U1378B 9H5	79.22		10.54

Table S2. Solid phase pyrite concentration and pyrite stable sulfur isotope (δ^{34}S-Pyrite) data for the upper 80 m sediments at IODP 334 Hole U1378B.

Sample	Depth [mbsf]	Pyrite [wt.%]	δ^{34}S-Pyrite [‰]
U1378B 1H1	1.68	0.41	-42.2
U1378B 1H2	3.18	0.32	-42.2
U1378B 1H3	4.68	0.53	-40.1
U1378B 1H4	5.08	0.45	-40.6
U1378B 2H1	6.98	0.60	-1.6
U1378B 2H2	8.3	0.88	-13.5
U1378B 2H3	9.98	0.72	-7.3
U1378B 2H4	11.48	0.98	1.6
U1378B 2H5	12.8	1.03	-4.2
U1378B 2H6	14.3	0.89	-5.1
U1378B 2H7	14.96	0.91	-6.6
U1378B 3H2	17.8	0.82	2.7
U1378B 3H3	19.28	0.65	-9.5
U1378B 3H5	22.28	0.60	-8.7
U1378B 3H6	23.73	0.68	-25.0
U1378B 4H3	27.89	0.86	-23.1
U1378B 5H2	36.78	1.17	-33.8
U1378B 6H2	46.28	1.06	-6.9
U1378B 7H2	55.78	1.06	-10.0
U1378B 8H2	63.92	0.83	-10.3
U1378B 9H2	74.83	1.08	-6.7

Table S3. Pore water sulfate stable sulfur isotope (δ^{34}S-SO4) and dissolved inorganic carbon (DIC) isotope (δ^{13}C-DIC) data for the upper 80 m sediments at IODP 334 Hole U1379C.

Sample	Depth [mbsf]	$\delta^{34}S\text{-}SO_4$ [‰]	δ^{13}C-DIC [‰]
U1379C 1H1	1.5	23.2	-4.13
U1379C 1H2	3	25.5	-6.41
U1379C 1H3	4.5	27.8	-9.63
U1379C 1H4	6	N/A	-10.66
U1379C 1H5	6.6	36.5	-9.66
U1379C 2H1	8.2	40.5	-9.91
U1379C 2H2	9.7	44.8	-10.73
U1379C 2H3	11.2	50.0	-9.84
U1379C 2H4	12.7	N/A	-8.08
U1379C 2H5	14.2	63.5	-10.47
U1379C 2H6	14.66	60.3	-10.25
U1379C 3H1	17.68	71.0	-12.12
U1379C 3H2	19.18	75.9	-12.37
U1379C 3H3	20.68	84.0	-11.68
U1379C 3H4	22.18		-12.28
U1379C 3H5	23.68		-12.34
U1379C 3H6	24.19		-12.36
U1379C 4H2	27.18		-12.07
U1379C 4H4	29.72		-12.21
U1379C 5H2	33.18		-11.58
U1379C 5H4	36.29		-12.25
U1379C 6H2	39.48		-12.54
U1379C 6H4	42.48		-10.89
U1379C 7H2	45.48		-10.67
U1379C 7H4	48.46		-9.12
U1379C 8H2	52.08		-8.96
U1379C 8H4	55		-8.72
U1379C 9H2	58.48		-7.59
U1379C 9H4	61.38		-6.35
U1379C 10H1	62.48		N/A
U1379C 11H1	64.98		-7.47
U1379C 11H3	67.38		-7.07
U1379C 12H2	70.68		-5.27
U1379C 12H4	73.33		-7.38
U1379C 13H2	76.68		-5.75

N/A – not analyzed

Table S4. Solid phase pyrite concentration and pyrite stable sulfur isotope (δ^{34}S-Pyrite) data for the upper 320 m sediments at IODP 334 Hole U1379C.

Sample	Depth [mbsf]	Pyrite [wt.%]	δ^{34}S-Pyrite [‰]
U1379C 1H1	1.5	1.36	N/A
U1379C 1H4	6	0.41	-14.8
U1379C 2H4	12.7	0.65	-28.2
U1379C 3H3	20.68	0.59	-39.3
U1379C 3H6	24.19	1.00	-34.4
U1379C 5H2	33.18	0.68	-20.0
U1379C 7H4	48.46	0.76	-28.3
U1379C 11H1	64.98	0.53	-26.6
U1379C 13H2	76.68	0.48	-19.1
U1379C 17H1	91.06	0.54	-26.3
U1379C 22X3	133.62	1.23	6.3
U1379C 24X6	158.79	0.37	-15.0
U1379C 27X6	188.08	1.10	-28.3
U1379C 30X2	211.63	1.59	-7.8
U1379C 33X5	243.52	0.89	-38.7
U1379C 37X5	282.78	1.69	-26.4
U1379C 41X4	320.48	1.34	-8.4

N/A – not analyzed

Table S5. Stable carbon (δ^{13}C-Carb), oxygen (δ^{18}O-Carb), and strontium isotopes ($^{87/86}$Sr) data for selected carbonates from IODP 334 Hole U1379C.

Sample	Depth [mbsf]	δ^{13}C-Carb [‰]	δ^{18}O-Carb [‰]	$^{87/86}$Sr
U1379C 15H-4	86.6	-18.27	4.40	0.70899
U1379C 16H-1	87.46	-16.31	3.94	0.70909
U1379C 19X CC	101.88	-25.51	3.47	0.70908
U1379C 22X-6	137.01	N/A	N/A	0.70897
U1379C 40X-1	306.1	-24.73	4.70	0.70911

N/A – not analyzed

References

Aloisi, G., Bouloubassi, I., Heijs, S.K., Pancost, R.D., Pierre, C., Damsté, J.S.S., Gottschal, J.C., Forney, L.J. and Rouchy, J.M., 2002. CH4-consuming microorganisms and the formation of carbonate crusts at cold seeps. *Earth and Planetary Science Letters*, *203*(1), pp.195-203.

Boetius, A., Ravenschlag, K., Schubert, C.J., Rickert, D., Widdel, F., Gieseke, A., Amann, R., Jørgensen, B.B., Witte, U. and Pfannkuche, O., 2000. A marine microbial consortium apparently mediating anaerobic oxidation of methane. *Nature*, *407*(6804), p.623.

Bohrmann, G., Heeschen, K., Jung, C., Weinrebe, W., Baranov, B., Cailleau, B., Heath, R., Hühnerbach, V., Hort, M., Masson, D. and Trummer, I., 2002. Widespread fluid expulsion along the seafloor of the Costa Rica convergent margin. Terra Nova, 14(2), pp.69-79.

Gieskes, J., Mahn, C., Day, S., Martin, J.B., Greinert, J., Rathburn, T. and McAdoo, B., 2005. A study of the chemistry of pore fluids and authigenic carbonates in methane seep environments: Kodiak Trench, Hydrate Ridge, Monterey Bay, and Eel River Basin. Chem. Geol., 220(3-4), pp.329-345.

Han, X., Suess, E., Liebetrau, V., Eisenhauer, A., and Huang, Y., 2014. Past methane release events and environmental conditions at the upper continental slope of the South China Sea: constraints by seep carbonates. International Journal of Earth Sciences, 103(7), 1873-1887.

Hesse, R. and Harrison, W.E. (1981). Gas hydrates (clathrates) causing pore-water freshening and oxygen isotope fractionation in deep-water sedimentary sections of terrigenous continental margins. Earth Planet. Sci. Lett., 55(3), pp.453-462.

Hong, W.L., Sauer, S., Panieri, G., Ambrose Jr, W.G., James, R.H., Plaza-Faverola, A. and Schneider, A., 2016. Removal of methane through hydrological, microbial, and geochemical processes in the shallow sediments of pockmarks along eastern Vestnesa Ridge (Svalbard). Limnology and Oceanography, 61(S1), pp.S324-S343.

Hong, W.L., Torres, M.E., Portnov, A., Waage, M., Haley, B. and Lepland, A., 2018. Variations in gas and water pulses at an Arctic seep: Fluid sources and methane transport. Geophysical Research Letters, 45(9), pp.4153-4162.

León, R., Somoza, L., Medialdea, T., González, F.J., Díaz-del-Río, V., Fernández-Puga, M., Maestro, A. and Mata, M.P., 2007. Sea-floor features related to hydrocarbon seeps in deepwater carbonate-mud mounds of the Gulf of Cádiz: from mud flows to carbonate precipitates. *Geo-Marine Letters*, *27*(2-4), pp.237-247.

Peckmann, J., Reimer, A., Luth, U., Luth, C., Hansen, B.T., Heinicke, C., Hoefs, J. and Reitner, J., 2001. Methane-derived carbonates and authigenic pyrite from the northwestern Black Sea. *Marine Geology*, *177*(1-2), pp.129-150.

Sahling, H., Masson, D. G., Ranero, C. R., Hühnerbach, V., Weinrebe, W., Klaucke, I., Bürk., D., Brückmann, W., and Suess, E., 2008. Fluid seepage at the continental margin offshore Costa Rica and southern Nicaragua. Geochem., Geophys., Geosyst., 9(5).

Teichert, B.M.A., Johnson, J.E., Solomon, E.A., Giosan, L., Rose, K., Kocherla, M., Connolly, E.C. and Torres, M.E., 2014. Composition and origin of authigenic carbonates in the Krishna–Godavari and Mahanadi Basins, eastern continental margin of India. Marine and Petroleum Geology, 58, pp.438-460.